Available online at www.CivileJournal.org

Civil Engineering Journal

(E-ISSN: 2476-3055; ISSN: 2676-6957)

Vol. 11, No. 03, March, 2025

An Automated Assessment Technique for Pavement Defects Using a Laser Scanner and Deep Machine Learning

Bara' Al-Mistarehi [1*], Amir Shtayat [2], Rana Imam [3], Ashraf Abdallah [4]

[1] Department of Civil Engineering, Jordan University of Science and Technology, Irbid 22110, Jordan.

[2] Department of City Planning and Design, Jordan University of Science and Technology, Irbid 22110, Jordan.

[3] Department of Civil Engineering, The University of Jordan, Amman 11942, Jordan.

[4] Department of Civil Engineering, Aswan University, Aswan 81528, Egypt.

Received 20 December 2024; Revised 09 February 2025; Accepted 17 February 2025; Published 01 March 2025

Abstract

Roads are vital arteries and main links between and within cities. They are considered the main auxiliary factor in shortening travel time and achieving users' comfort and safety. Governments strive to provide ideal conditions on the roads to achieve the highest levels of satisfaction, which are reflected in the quality of rides provided. Despite the variety of monitoring and evaluation methods, achieving the best and most accurate diagnosis of the condition of the roads and determining the severity of defects and appropriate and rapid maintenance methods are still lacking. This study aims to monitor and evaluate the state of some roads in Aswan City, Egypt, to identify defects and address them promptly. To achieve this goal, a laser scanner was used to evaluate pavement conditions by measuring the coordinates of the road surface and determining the differences in the measured values on the three axes. A built-in camera was also used in the laser device to monitor the type and severity of defects and match them with the measurements of the laser scanner device. Finally, a deep machine learning system, including LSTM, GRU, RF, SVM, and DT, was used to identify and classify the type and severity of defects. The prediction models showed significant accuracy with about 93%, 91%, 85%, 84%, and 82%, respectively.

Keywords: Pavement Condition; Defects; Prediction; Laser; Machine Learning.

1. Introduction

Highways are a fundamental element of industrialized societies. They serve a crucial function in connecting cities, districts, states, and even nations. The frequent and substantial vehicular stress on roadways typically results in surface flaws in the pavement. Pavement flaws are typically referred to as distresses, which are classified into many categories that affect both the quality and roadway performance. These distresses could be assorted and described as follows: cracking, which is the predominant distress type on primary roads, whereas minor roads suffer more from pits, patches, and rutting [1-4]. In fact, there are nineteen varieties of distress that are present in flexible pavement. Nevertheless, the main focus of this investigation is to evaluate and assess longitudinal fractures and rutting.

In order to maintain the functionality of roadways, it is imperative to conduct routine maintenance that is based on precise pavement observations and surveys. Professionals who are capable of observing, capturing images, gathering data, and evaluating road distresses can conduct this type of inspection. This conventional method of data

* Corresponding author: bwmistarehi@just.edu.jo

http://dx.doi.org/10.28991/CEJ-2025-011-03-015

collection is characterized by numerous limitations and drawbacks, including its tendency to be time-consuming, labor-intensive, and hazardous, particularly on highways, and its susceptibility to personality. [1, 5-8]. Accordingly, for almost 50 years, numerous researchers have implemented automatic distress data collection through digital imaging technology. This approach mitigates the hazards to human evaluators and the inconvenience to traffic during the survey [9]. High-speed complementary metal–oxide–semiconductor (CMOS) industrial cameras were used by Zhang et al. (2014) [10] to automatically detect cracks in a subway tunnel by applying thresholding operations and the technique of morphological image processing, while Zhang et al. (2016) [11] employed neural networks to detect road pavement cracks. Shatnawi (2018) [12] analyzed images captured by drones with neural networks to identify pavement distresses on secondary roads.

Laser scanning is an automated, direct measurement of three-dimensional points, as opposed to image-based methods [13]. The Mobile Mapping System (MMS) is often classified into either laser-based or image-based [14]. In transportation mapping and surveying, image-based mobile mapping has significantly enhanced traditional evaluation, such as the assessment of roadway borders for roadway safety support and modeling [15, 16]. This noteworthy advantage is due to the nature of photos containing texture and vibrant color information, which facilitates road recognition and automated distress extraction. Al-Durgham et al. (2021) [17] provided a computerized approach for assessing the level of accuracy and quality of cloud data obtained from mobile mapping systems utilizing consumer-grade microelectromechanical systems (MEMS) sensors with portable laser scanners. The study's conclusions demonstrated a high degree of accuracy suitable for the precise evaluation of mobile mapping systems.

A wide range of transportation applications, including automatic road distress extraction, model-based road design, and monitoring, have been made possible by the development of 3D laser scanning technology. Compared to photogrammetry and field inspections, laser scanners could gather extremely precise point clouds in three dimensions that have high density over a short period of time [18]. Additionally, laser scanner systems give additional implicit data, including scanning patterns, intensity, and rutting depth, which all contribute to road extraction, in addition to collecting clear, extremely precise elevation information. In addition, the use of LIDAR data for road environment monitoring and road fault detection has grown in recent years. The high point density LIDAR data sets may be used to derive rut depths [19]. It is possible to color LIDAR point clouds, which might provide some insight into the locations of ruts from data sets with lower point densities. Laser scanning technology may be used to acquire precise and efficient rutting data at the network level for different highway speeds [20]. Obaidat et al. (2020) [21] employed a highly accurate positioning system (RTK) and a smartphone to evaluate rutting on secondary roads in the north of Jordan. Additionally, rutting and lateral displacement models were developed using a variety of characteristics, including lane width, truck percentage, pavement age, pavement thickness, and annual average daily traffic (AADT). The study found that, in comparison to the manually operated process utilizing Root Mean Square error (RMSE), the adopted approach provided accurate and fair findings. Data collection by laser technologies on highways is best performed at light to medium traffic conditions; avoiding rush hours is advised. In summary, compared to human techniques, laser scanning technologies are more useful for longitudinal cracking and rut depth measuring. On the other hand, these technologies reduce the data collection time and safety risks on site, yet they are accurate.

The fractured pavement has distinct textural qualities. Most studies obtain the texture elements of photos from diverse locations and use machine learning classification methodology to automatically extract fractured pavement. Hu et al. (2010) [22] proposed an automated fracture pavement extraction approach based on form and texture descriptions. It is concluded that the texture of the fractured pavement is uneven. So, the study report recommended using two translation-invariant shape descriptors and six texture features to portray the picture's irregular texture and uneven lighting properties, followed by an SVM classifier to categorize the image as cracks or no cracks. Cord & Chambon (2012) [23] utilized a universal crack detection algorithm based on supervised learning, which may be used for any type of distress in those pictures.

The research concluded that fractures in pavement require substantial texture information. The textural elements of the fracture pavement exhibit two behaviors: (1) varying within the local range; (2) demonstrating homogeneity over the global range. As a result, this research employs linear and nonlinear filters to analyze the texture of images. Morphological transition, linear filtering, and non-linear filtering were all employed to examine picture attributes at various scales. Finally, the AdaBoost classifier was used to learn and categorize the aforementioned textural information, as well as to determine the extent of pavement damage. Finally, while this technology improves crack extraction efficiency up to a point, it is unable to identify fine crack extraction. Shi et al. (2016) [24] present the crack forest approach, which uses a random structure forest to extract asphalt fracture pavement.

The intensity-thresholding methodology has been extensively proposed for fracture detection [25-28]. However, the background illumination and pavement texture had a substantial impact on the performance of this methodology, resulting in an ambiguous crack segmentation. The OTSU algorithm is frequently implemented by researchers in the context of low noise-signal image ratio [29]. Satisfactory detection results can be achieved through the implementation of an effective segmentation algorithm [30, 31]. A histogram-based classification algorithm was proposed by Prasanna

et al. (2012) [32] and was combined with Support Vector Machines (SVM) in order to extract fractures on the concrete surface. The outcomes indicated that the precision of practical predictions needed to be upgraded. Hoang & Nguyen (2019) [33] conducted a comparison of various machine learning-based classification algorithms. The findings indicated that the maximum accuracy level of classification was achieved by SVM (80.50%), followed by ANN (84.25%), and then RF (70%). Gavilan et al. (2011) [34] proposed a road fracture detection system that utilized Support Vector Machine (SVM). The results indicated that a linear SVM classifier could differentiate amongst ten varieties of pavements that are present on Spanish roads. The segmentation methodology of the SVM-based method considers neighboring pixel information.

Chen et al. (2022) [35] reviewed the computer vision techniques, from image processing to machine learning methods, across different challenge-focused works of automatic road damage detection. The different classifications of road defects were identified, and the most up-to-date data collection technologies were discussed. Finogeev et al. (2024) [36] developed an approach to detect and classify pavement defects in images of road sections obtained from photographs and video frames in the process of road scanning and Deep Machine learning methods. This approach includes two methods: a) a method using IoU-HOG-ACM-BoVW algorithms for recognition and classification of high noise images; b) a method of segmentation and recognition using convolutional neural network MaskR-CNN for recognition and classification of low noise images. The algorithms were used for solving the problems of segmenting road pavement images into parts with detected damages, determining the boundaries and geometric dimensions of defects, classifying damages by type, and clustering and ranking road segments according to the operational condition of the road pavement. Hassan et al. (2022) [37] proposed an automatic patch detection system using object detection techniques and advanced pavement inspection systems such as LCMS (Laser Crack Measurement System). Results showed that the object detection model can successfully detect patches inside LCMS images and suggested that the proposed approach could be integrated into the existing pavement inspection systems. Mihoub et al. (2023) [38] provided a novel application for data collection regarding road states, entitled "Road Scanner". It allows onboard users to tag four types of segments in roads: smoothness, bumps, potholes, and others. For each tagged segment, the application records multimodal data using the embedded sensors of a smartphone. The collected data concerns mainly vehicle accelerations, angular rotations, and geographical positions recorded by, respectively, the accelerometer, the gyroscope, and the GPS sensor of a user's phone. Moreover, a medium-size dataset was built, and machine learning models were applied to detect the right label for the road segment. The results were very promising since the SVM classifier (Support Vector Machines) recorded an accuracy rate of 80.05%.

Cui et al. (2024) [39] adopted a semi-supervised learning approach to train ResNet-18 for image feature retrieval and then classification and detection of pavement defects. The resulting feature embedding vectors from image patches were retrieved, concatenated, and randomly sampled to model a multivariate normal distribution based on the only one-class training pavement image dataset. The calibration pavement image dataset was used to determine the defect score threshold based on the receiver operating characteristic curve, with the Mahalanobis distance employed as a metric to evaluate differences between normal and defect pavement images. Then, a heat map derived from the defect score map for the testing dataset was overlaid on the original pavement images to provide insight into the network's decisions and guide measures to improve its performance. The results demonstrate that the model's classification accuracy improved from 0.868 to 0.887 using the expanded and augmented pavement image data based on the analysis of heatmaps. Another method was proposed by Daneshvari et al. 2024 [40] to detect asphalt pavement bleeding using a one-class support vector machine (SVM) algorithm, with a reported F1-score of 80.29%.

Han et al. (2024) [41] introduced a two-stage segmentation framework to detect pavement cracks using both supervised and unsupervised strategies, reporting that their model surpassed other state-of-the-art neural networks in intersection over union (IoU) scores. Isradi et al. (2024) [42] applied the Markovian probability operational research process to develop a decision support system for predicting future pavement conditions. The process determines effective policies for managing and maintaining roads by observing the history of pavement damage from year to year to estimate the transition probability as a Markovian-based performance prediction model. The results showed that the application of the model was optimal. Changes in pavement condition after applying the maintenance plan resulted in the good condition reaching 92.8% and a stable condition for 95.72% of the pavement by the end of the design life.

Zafar et al. (2019) [43] categorized the common types of distress that exist on "Lakhi Larkana National Highway (N-105)" to estimate the pavement condition index. Using this data, the average PCI for the highway section was calculated. to assess the pavement performance; 10 out of 19 defects were recognized in the pavement, as stated by the PCI method. Results indicated that the common pavement distress types were depressions, polished aggregate, rutting, potholes, block cracking, and alligator cracking. One-Class Support Vector Machine (OCSVM), which is an anomaly detection approach, could be beneficial for classifying images of bleeding asphalt. Computer vision techniques are used to extract efficient features, which serve as inputs for the OCSVM model. In order to evaluate the suggested model's performance, two separate imbalanced datasets of images are utilized to train and test the model. Finally, in terms of F1-Score, the OCSVM achieved 97.29% in the testing dataset [44]. This latter research aimed to achieve pixel-level

detection of pavement cracks and proposed the two-stage Crack Diffusion framework, which combines unsupervised and supervised learning to achieve superior performance in crack detection. On four public datasets, both the proposed multi-blur-based cold diffusion model and the comprehensive Crack Diffusion framework attained the highest Intersection over Union (IoU) scores, surpassing the IoU scores of the current state-of-the-practice unsupervised and supervised segmentation models [41].

Based on 3D laser scanning pavement data, an automatic defect detection method is proposed by Zhang et al. (2018) [45] to detect pavement cracks and pavement deformation defects information simultaneously. The experimental results showed that, based on the 3D laser scanning data [46], the proposed method could effectively detect typical cracks under different road conditions and environments, with the detection accuracy above 78%. Furthermore, different types of deformation defects, including potholes, rutting, shoving, and subsidence, were accurately detected with a location error of less than 8.7%.

Azam et al. (2023) [47] proposed an effective assessment method for the evaluation of flexible pavement surface distresses using Terrestrial Laser Scanner (TLS). The evaluation was carried out to assess different types of pavement distress such as cracking, rutting, roughness, and miscellaneous distresses. Every pavement distress was defined in terms of surface area, width of crack, and intensity; then the data from TLS was processed by MAGNET COLLAGE software. Hereafter, a designed MATLAB program was developed to match the 26 TLS observational data to plane equations. The revealed distresses for the investigated road using TLS observations reveal a significant improvement in determining flexible pavement distresses and geometric characteristics.

The intelligent detection of pavement distress using deep learning methods has consistently been a hot topic in pavement maintenance. Zheng et al. (2024) [48] aimed to offer new insights to promote research and application in this field through bibliometric analysis. Riid et al. (2018) [49] employed deep learning convolutional neural network models towards the implementation of the detector and introduced a manual preprocessing step: sets of orthoframes are carefully selected for training and manually digitized to ensure adequate performance of the detector. Pretrained convolutional neural networks are then fine-tuned for the problem of pavement distress detection. Corresponding experimental results are provided and analyzed and indicate a successful implementation of the detector.

It is obvious that there are different methodologies for distress detection and classification, like laser scanner and image processing techniques, deep machine learning, and traditional PCI procedures. Every methodology has its own unique performance, accuracy, and standard deviation based on different factors like the type of distress to be detected, the methodology itself, and the drawbacks/limitations associated with it. In conclusion, it is considered case dependent. The novelty of this research lies in investigating the integration between potential terrestrial laser scanning systems, deep machine learning prediction models, and validation using the standard PCI procedure based on the PAVER system for automated prediction, detection, and classification of longitudinal cracks and rutting using actual flexible pavement data from the case study highways in Egypt. The present research aims at:

- Using the laser scanner as a monitoring device to identify coordinates (x, y, z) of the longitudinal cracks and rutting in order to quantify and describe qualitatively the pavement cracks along the road sections. Besides, an attempt is made to extract the changes in coordinates to understand the pavement cracks and their behavior along the road surface.
- Building and developing five deep-learning prediction models to predict, detect, and classify road conditions based on laser scanner data, including Long Short-Term Memory (LSTM), Gated Recurrent Unit Network (GRU), Random Forest (RF), Support Vector Machine (SVM), and Decision Tree (DT). The selected prediction models focus on deep learning of the behavior and performance of single and sequential data related to the road pavement condition. In this study, three main defect classes were taken into consideration in the deep learning prediction models: 1) normal (ideal pavement spots), 2) longitudinal cracks, and 3) rutting. All of these defects were visually monitored and measured using the laser device.
- Evaluating pavement distress conditions located on the selected roads of Aswan City using the standard PCI procedure based on the PAVER system for validation purposes.

2. Data

In this section, all data information and details are presented, including site locations, data collection procedures using a laser scanner and pavement condition index, and data analysis. Figure 1 shows the workflow of this research.

2.1. Description of Case Study Areas

Two study areas have been scanned in New Aswan City, which is located in the south of Egypt with a latitude of (24.15958° N – 24.21470° N) and a longitude of (32.83939° E– 32.86710° E). In Figure 3, the left photo presents the layout of New Aswan City, whereas the top right photo presents the first study area location in front of the Faculty of Islamic Studies for Girls in Al-Azhar University, and the bottom right one shows the second location opposite Bank Misr.

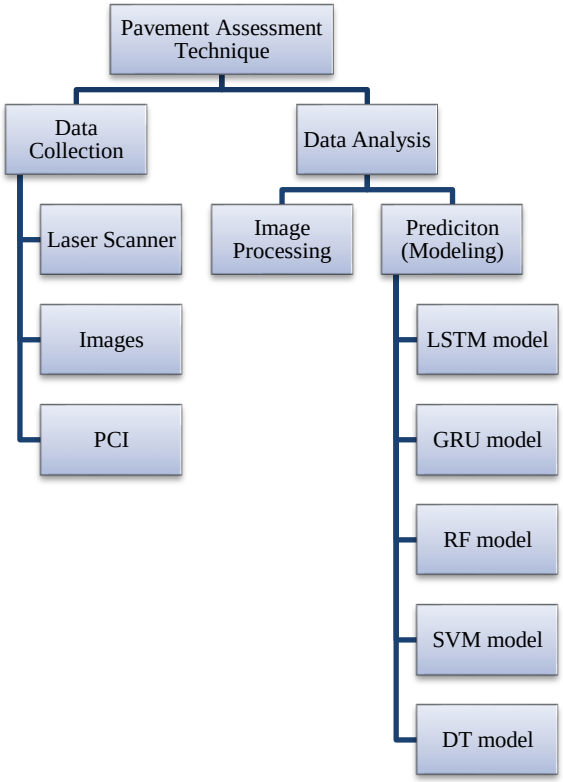

Figure 1. The study workflow

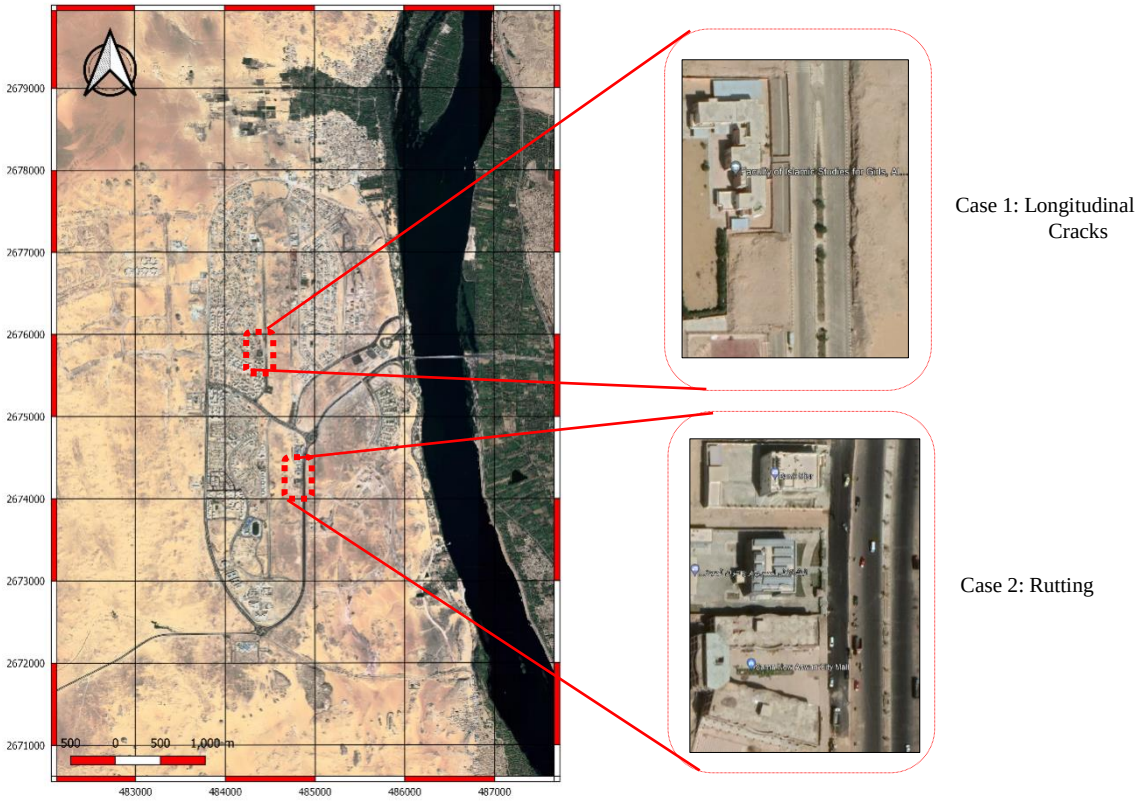

Figure 2. Location of the study areas: New Aswan City, Egypt

2.2. Data Collected by the Laser Scanner

A terrestrial 3D laser scanner of FARO FOCUS S has been used to obtain a 360-degree view designed to give an accurate position of every pixel in point cloud format. It is a panoramic scanner that is integrated with a tilt sensor, barometer, and a magnetic compass. Table 1 describes the technical details of the scanner [46].

Table 1. Technical specifications of the Faro Focus3D S120 laser scanner

Architecture	Panoramic
HFOV/VFOV	360º/305º
Range measurement principle	Phase-based
Maximum Scan rate	976 000 Hz
Unambiguity interval	153.49 m
Spot size	3.8 mm + 0.16 mrad
Range precision @ 25 m (90% albedo)	0.95 mm (0.50 mm)
Range accuracy @ 25 m (90% albedo)	± 2 mm
Weight	5 kg
Size	240 x 200 x 100 mm
Operating temperature	5oC-40oC
Levelling sensor	Dual-axis tilt sensor
Heading sensor	Electronic compass
Height sensor	Barometer
RGB	Built-in camera

As shown in Figure 3, the successive stages of terrestrial laser scanning (TLS) procedure are as follows:

- Specifying the scanning parameters [image resolution and point cloud density].
- Distributing the black-white checkboards [targets] for data registration later (refer to Figure 4-b).
- Acquiring the point cloud data using the laser scanner with high resolution (Resolution ¼ & Quality 4X, which means 6 mm / 10 m). It is preferred to be no more than 5m away from the crack to obtain 3 mm distance between scanned points.
- Registering the scans using FARO SCENE software. The scans had an overlap between 86 – 96% with point error between 1.1-1.7 mm. Further, the registered data was performed in the laser scanner local system.
- Extracting the oriented data to the suitable format [.e57, .las, and Recap format].

Figure 3. Successive stages of the terrestrial laser scanning (TLS) procedure

2.2.1. Case Study 1: Longitudinal Cracks

As seen in Figure 4, the pavement in front of the Faculty of Islamic Studies for Girls, Al-Azhar University, has been scanned to obtain the three-dimensional coordinates of the longitudinal cracks. Figure 4-a depicts the 3D laser scanner during the scanning of the longitudinal cracks in New Aswan City. Figure 4-b shows the onsite target for data registration using FARO SCENE software, whereas Figure 4-c presents a real photo of the cracks. More than 1.2 million dense points were scanned onsite, as shown in Figure 4-d.

2.2.2. Case Study 2: Rutting Cracks

Figure 5 shows the details of the rutting cracks of the case study. Figure 5-a shows the 3D laser scanner during the scanning of the rutting area. The condition of the pavement distresses due to the rutting was measured manually as depicted in Figure 5-b. The selected section for evaluation has more than 4.5 million 3D point clouds. Figures 5-c and 5-d are the plan and cross-section of the point clouds generated using the CloudCompare software.

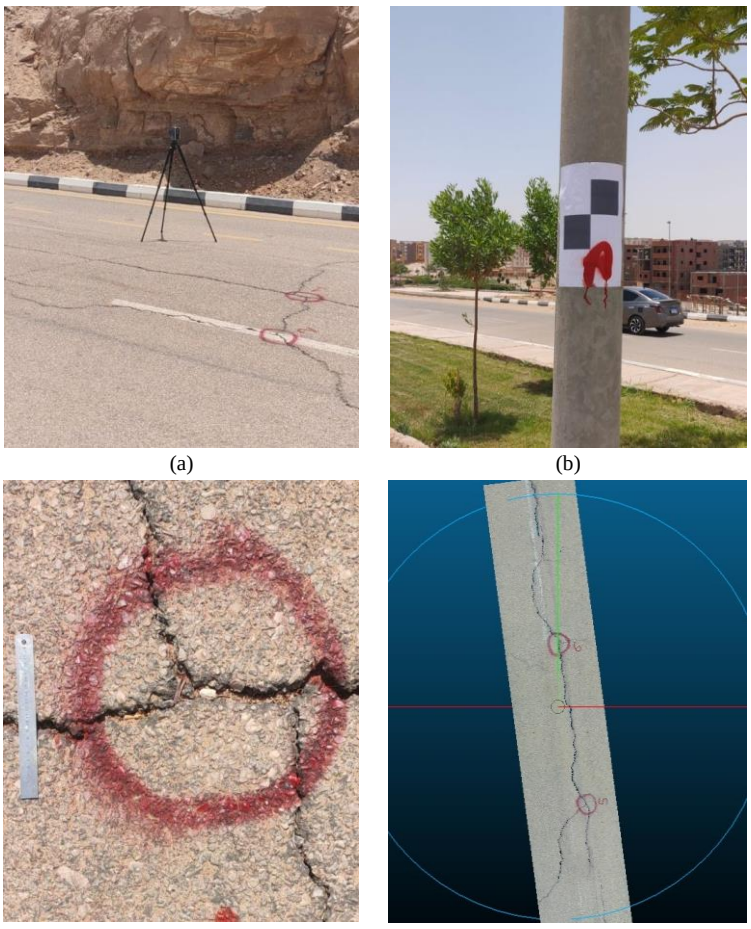

(a) (b)

(c) (d)

Figure 4. Scanning details of the longitudinal cracks

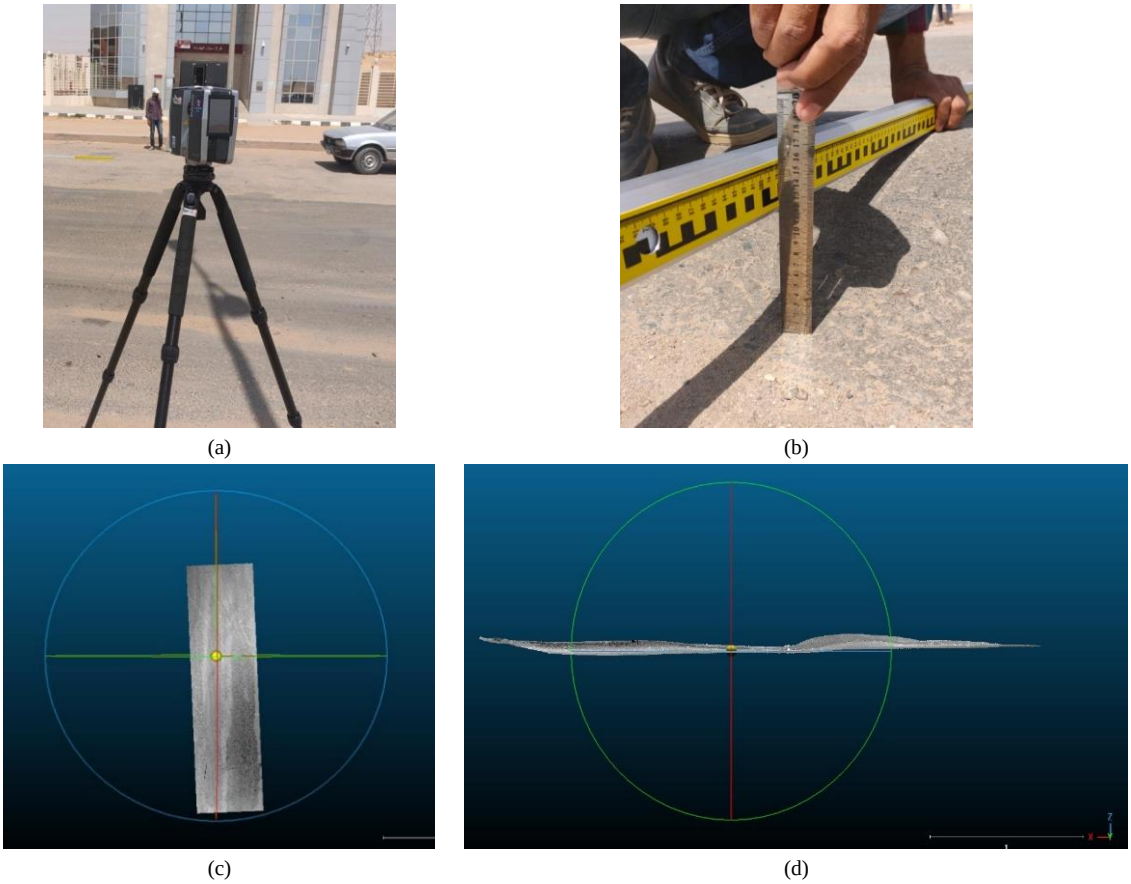

(a) (b)

(c) (d)

Figure 5. Scanning details of the rutting cracks

2.3. Data Collection and Evaluation using PCI

The PCI was calculated using the findings from a visual condition assessment that determined the kind, severity, and quantity of discomfort. The PCI was created to serve as an indication of the pavement's structural integrity and surface operating condition. The designated roads in Aswan city were categorized into branches, determined as recognizable segments of the pavement network that serve as singular entities with certain roles. The chosen branches are subdivided into smaller units referred to as sections. The subsequent variables were evaluated while partitioning branches into fields:

- Pavement structure: the structural formulation, including thickness and materials.
- Traffic: the quantity and severity of vehicular movement.
- The pavement components must possess identical construction histories.
- Pavement Rank: the functional categorization (arterial, collector, or local).
- Drainage facilities: the drainage systems and shoulders must be uniform over the pavement length.

The database contained three asphalt pavement sections (5 m in total) of the roadway network in Aswan city: the "Normal" (perfect pavement places) section, the longitudinal fractures section, and the rutting section. The three pavement portions were randomly split into units of 232 ± (10) m². The minimum number of sample units to be examined for asphalt concrete AC surfaced pavements is decided based on the whole number of sample units and the PCI standard deviation, which is considered to be 10. The Normal (ideal pavement spots) section was divided into 5 random sample units, the Longitudinal cracks section was divided into 15 random sample units, and the Rutting section was divided into 10 random sample units [50]. A hand odometer was used to measure the length and size of each disturbed patch. A straight edge and ruler were used to determine the extent of ruts or depressions. The distress inspection was carried out by walking across the sample unit, manually categorizing distress types based on observation and visualization, and quantifying distress quantity with a tape and hand odometer. The distress intensity levels were manually assessed using visualization and the distress criteria outlined in the PCI distress handbook and PAVER System; these criteria differ depending on the type of distress encountered. The severity degree of a distress is a rating index that categorizes the distress into three sorts depending on different ranking criteria. There are three severity levels: low, medium, and severe. The general elements that determine the severity level of numerous cracks include: 1. Crack width. 2. The crack's state, including whether it was previously filled or not. 3. Various fractures surrounding the crack. 4. The condition of the region surrounding the fracture [50]. Finally, the gathered data were entered on the flexible pavement survey sheet for each sample unit; the Micro PAVER 5.2 version was released by inputting the distress type, quantity, and severity for each sample unit in section 1; and PCI and PCI rating were computed automatically, as shown in Table 2.

Table 2. The collected data for PCI evaluation

Section Parts	Number of Sample Unit	Type of Sample Unit	Area of Sample Unit	Distress Number	Distress Description	Distress Severity Level	Quantity	Unit of Quantity	PCI for each sample unit	PCI Rate
Normal (ideal pavement spots) Part 1	1	Random	230	m^2	No Distress	-	0	-	100	Good
	2	Random	230	m^2	No Distress	-	0	-	100	Good
Longitudinal cracks Part 2	1	Random	230	m^2	Longitudinal crack	L	0.3	m	50	poor
					Alligator cracking	M	0.8	m^2		
					Bleeding	H	0.2	m^2		
					Edge cracking	H	1.2	m		
	2	Random	230	m^2	Block cracking	H	1.7	m^2	35	Very poor
					Bumps	L	0.5	m		
					Longitudinal crack	M	0.4	m		
					Pothole	H	1	number		
					Patching	M	0.9	m^2		
					Polished aggregate	M	1.5	m^2		
					Block cracking	H	1.7	m^2		
Rutting Part 3	1	Random	230	m^2	Rutting	H	0.5	m^2	53	Poor
					Pothole	L	2	number		
					Polished aggregate	M	1.7	m^2		
					Block cracking	M	2.4	m^2		
	2	Random	230	m^2	Polished aggregate	M	2.0	m^2	28	Very poor
					Alligator cracking	H	2.5	m^2		
					Pothole	H	1	number.		
					Rutting	L	0.2	m^2		

2.4. Data Analysis

This section describes the created models, which include LSTM, GRU, RF, SVM, and DT, for predicting, detecting, and classifying pavement fault data gathered by a laser scanner. The prediction model was built using scanned data separated into training and testing sets in proportions of 70% and 30%, respectively. Python software was used to build and develop the prediction models, which were subject to rigorous quality control and operation. Table 3 displays the acquired laser data for pavement abnormalities on chosen road segments in Egypt. The results revealed a sample of the laser measurements taken in a damaged area with longitudinal fractures. The laser scanner determined the coordinates (x, y, z) of longitudinal fractures and rutting in order to quantify and subjectively describe pavement cracks along road sections. Aside from that, an attempt was made to extract coordinate changes in order to better understand pavement cracks and their behavior on the road surface. In Table 3, the first three columns summarize the coordinates, while columns 4-6 show the color intensity of the point clouds.

Table 3. Collected data by the laser scanner

X-axis	Y-axis	Z-axis	Red	Green	Blue
0.2313	-5.1021	66.2135	170	174	160
0.2367	-5.0989	66.2137	152	156	148
0.2319	-5.1061	66.2151	172	175	162
0.2349	-5.1038	66.215	164	167	155
0.2322	-5.0999	66.2154	163	166	154
0.2366	-5.1026	66.215	154	158	149
0.2344	-5.0995	66.2158	157	160	150
0.2406	-5.1046	66.2142	158	158	154
0.2429	-5.1037	66.2144	160	159	157

The data showed differences in the x, y, and z axes. Nevertheless, according to the visual inspection and captured images from the field (refer to Figures 6-a to 6-c), the changes in the data resulted from anomalies on the selected road pavement. Basically, the differences in x values indicated offsets in the pavement surface to the left or right, which means an event (defect) existed on the pavement surface with a specific width. More clearly, the width of defects was represented to be measured on the x-axis. On the other hand, the y-axis represented the length of the defects. At the same time, the z-axis was more significant in terms of identifying the depth of the cracking and rutting.

Figure 6 presents different cross-sections of the longitudinal cracks located at the selected road in Aswan. Figure 6-a shows four different cross-sections captured to be later analyzed and plotted to understand the behavior profile. In Figure 6-b, the heat map technique was applied to the laser scanner data using MATLAB to identify and detect the exact edges of the cracks along the road segment. As shown in Figure 6-c, the cross-section profile of the longitudinal crack in the selected section was plotted using the data in Table 3. The x-axis data represents the road section width, which could also describe the width of the cracks. In contrast, the z-axis represents the elevation of the road surface, which highlights pavement defects and their depth. According to Figure 6-c, the graph indicates a slight depression to the right, which can be interpreted as the natural slope of the road for drainage purposes.

However, approximately 3.5 to 6.0 m from the width of the road, a sharp drop was noticed in the road level, which was interpreted as a defect in the road surface. The subsidence on the cross-section profile indicated that a longitudinal crack was detected and identified after matching the laser data and captured images. On the other hand, Figure 6-d presents the cross-section profile of the selected segment, indicating the transverse length of the rutting on the cross-sectional road surface. Moreover, the elevation of the road surface was taken into consideration as shown in the vertical axis. A slight to moderate subsidence could be noticed in the selected segment. This subsidence indicates that there was rutting at that section with a transverse length of about 1 m and a depth of 2 cm.

A matching process was also performed among collected laser scanner data, captured images, and PCI data to identify the location, type, and severity of each pavement distress type, as shown in Figures 7 and 8 for longitudinal cracks cross sections and rutting cross sections, respectively.

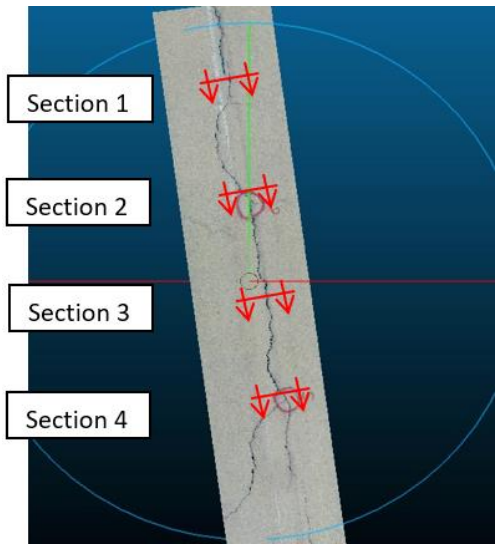

(a)

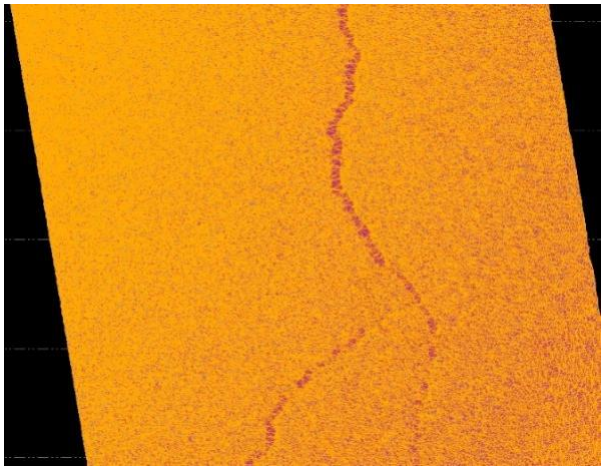

(b)

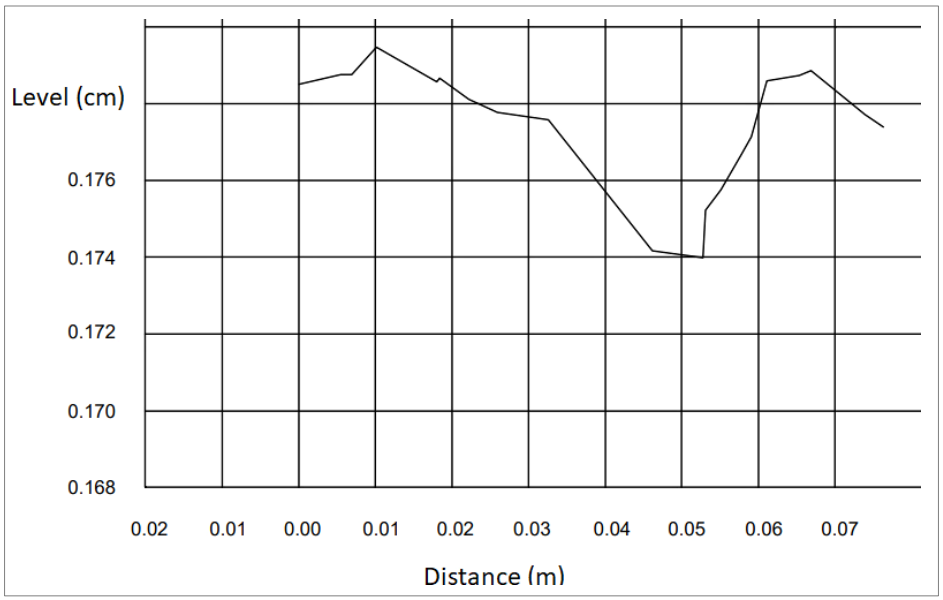

(c)

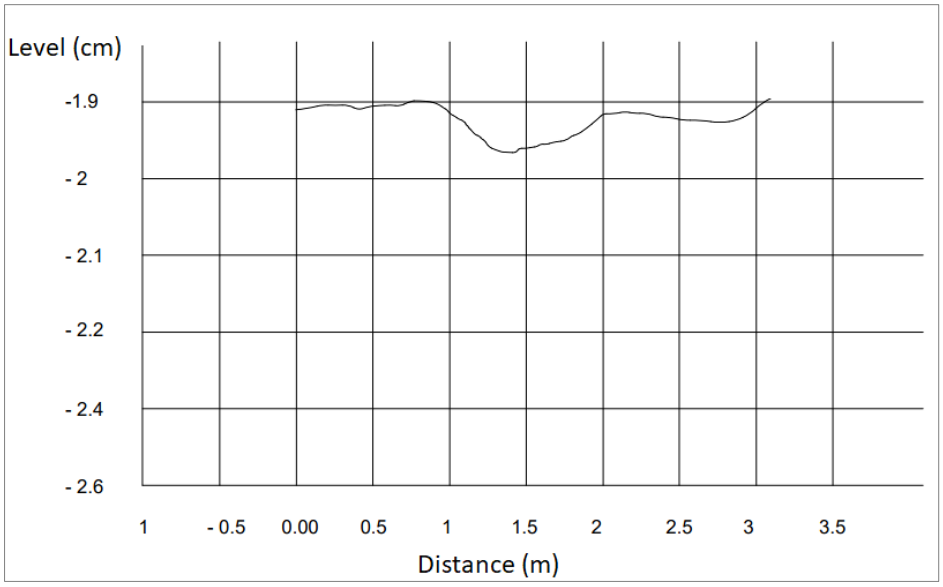

(d)

Figure 6. (a) Longitudinal crack cross-sections; (b) Longitudinal crack heat map; (c) Longitudinal crack profile; (d) Rutting profile

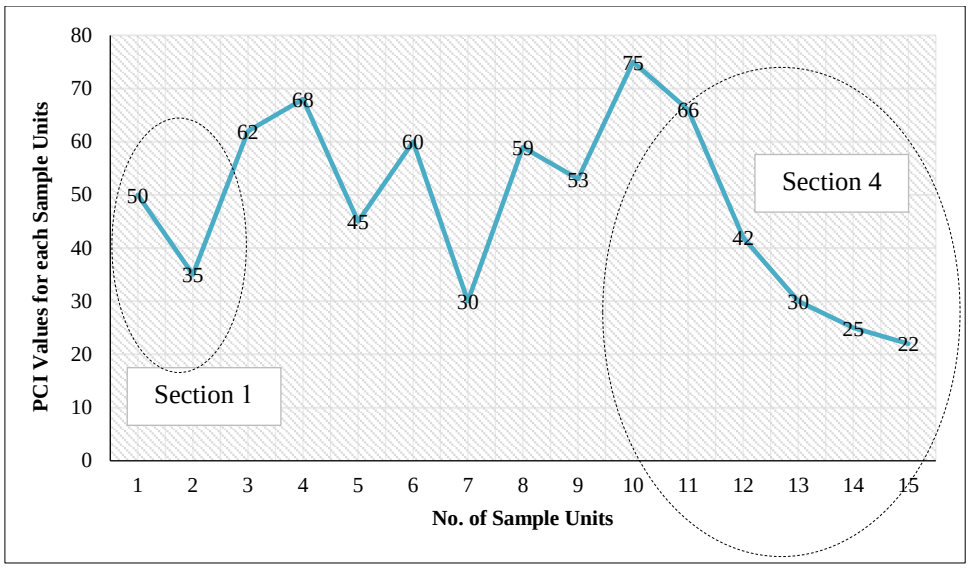

Figure 7. PCI values for longitudinal crack cross-sections

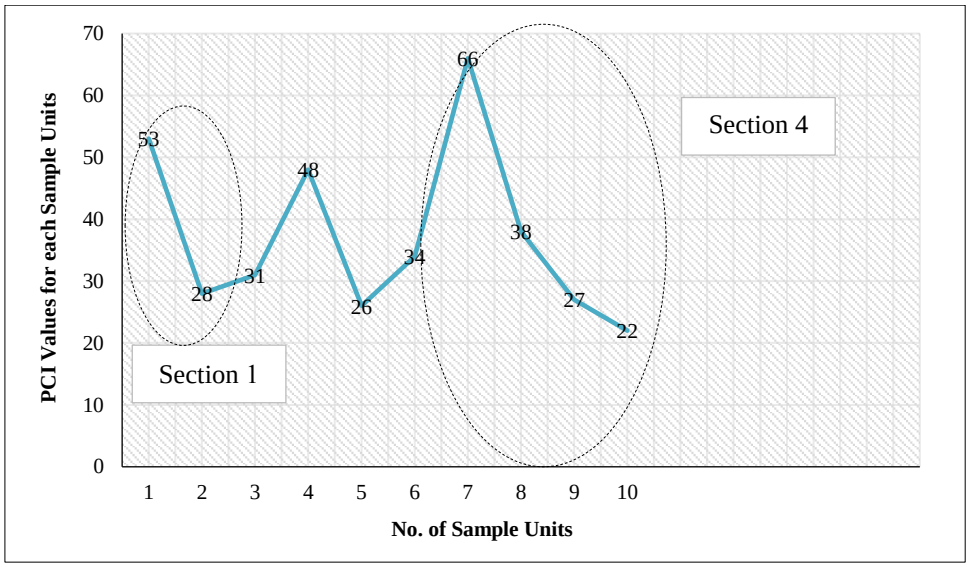

Figure 8. PCI values for rutting cross-sections

Figure 7 presents the trend and relationship between the number of sample units and associated PCI for each sample unit for four different cross-sections of the longitudinal cracks located at the selected road in Aswan city. Figure 7 was plotted using the collected visual inspection data for PCI Evaluation from Table 2, where the x-axis data illustrates the number of sample units. At the same time, the y-axis describes the PCI for each sample unit, which can easily give an indication about the situation of the pavement. Based on the drawing, the sample units No. 1 and No. 2 represent section 1, the sample units from No. 11 to No. 15 represent section 4, while the remaining sample units from No. 3 to No. 10 were distributed between sections 2 and 3. In general, the curve of sections 1 and 4 indicates a slight depression and drop with the values of the PCI (down from 50 to 35 for section 1; from 66 to 22 for section 4), which is interpreted as the presence of defects and problems in the road surface. According to Shahin et al. [3], the PCI rate was rated as "Poor" at a PCI value of 50 and then dropped to a PCI value of 35 with a rating of "Very Poor". The same drop in PCI values occurred in section 4, where the PCI rate was (Fair) at PCI value (66) and dropped to (Very Poor and Serious) at PCI values (25) and (22), respectively, for the last two sample units of section 4. The same comparison for rutting cross sections was done using Figure 7.

Figure 7 was plotted based on Table 2 between the number of sample units (x-axis) and PCI for each sample unit (y-axis). Sample units No. 1 and 2 represent section 1, while section 4 is shown by the sample units (7, 8, 9, and 10). The situation for rutting data showed that there is a depression and drop in the values of the PCI, like the longitudinal cracks. The PCI rate was poor at PCI value (53) and then dropped to PCI value (28) with a rating of (very poor). The same drop for the PCI rate occurred at section 4, where the PCI rate was (fair) at PCI value (66) and approximately dropped to (serious) at PCI values (22) for the last sample unit of section 4. The reason for the drop of PCI of longitudinal cracks and rutting cross sections is due to the existence of other types of distresses with high and medium severity levels in the

same area of longitudinal cracks or rutting as seen in Table 2. This situation decreased the values of the PCI, and the pavement became worse. This means that this pavement needs maintenance and repair. In conclusion, the results from Figures 7 and 8 are consistent and in agreement with collected laser scanner data and captured images for the validation process. As for determining the shape of cross-sections, the output of laser-measured data proved that the use of laser scanner technology gives a great opportunity to increase the efficiency of road condition assessment and to identify the location, type, and severity of defects in the pavement surface. Besides, defects can be represented in a three-dimensional image, through which the severity of defects can be automatically determined with high accuracy. Thus, all dimensions of defects can be identified.

Before applying the prediction models to the scanned data, pre-processing techniques were performed in order to prepare, organize, and manage the data for detection and classification processes. The data were manually labeled into three main groups: normal, cracking, and rutting. Normal data indicates that the pavement was in an ideal condition and no defects had been measured. In comparison, the other groups were identified using images from the same laser device and visual inspection reports. After that, an attempt was made to extract samples of the data to be tested using the selected prediction models and used later for training the models.

3. Results and Discussion

Pavement defects play a crucial role in the deterioration of the road service condition and, thus, its inability to provide comfort to road users. It may also cause economic losses due to damage to vehicles and human losses due to poor road conditions. To achieve permanence and sustainability of the road condition, many researchers resort to exploring how to monitor the road condition and then develop appropriate prediction models to determine the road performance over the operational life of the road. Likewise, many researchers use prediction models that focus heavily on identifying and classifying road defects automatically based on digital data in all its forms, whether images, vibration data, or laser data. In this study, three main defect classes were taken into consideration in the deep learning prediction model: 1) normal (ideal pavement spots), 2) longitudinal cracks, and 3) rutting. All these defects were visually monitored and measured using the laser device. Regarding data, 70% of the datasets were trained, and 30% were tested for each model development process. In addition, other data samples from the laser were trained using the selected models to keep them ready for later validation and testing. Table 4 shows the performance of the selected prediction models in detecting and classifying longitudinal cracks using a laser scanner.

Table 4. Detection and classification of the longitudinal cracks using deep learning models

Model name	Precision	Recall	F1 score	Accuracy
LSTM	92.97	91.38	92.17	94.67
GRU	91.37	90.32	90.84	92.37
RF	85.35	82.93	84.12	85.83
SVM	84.77	83.82	84.29	84.19
DT	83.86	81.22	82.52	82.55

Table 4 presents the effectiveness of deep-learning prediction models, including LSTM, GRU, RF, SVM, and DT, in foretelling pavement conditions. The models' results show significant performance in detecting and classifying the longitudinal cracks among different distress types located at the selected road segment surface. More clearly, the artificial neural network models, including LSTM and GRU, show excellent accuracy in detecting and classifying the longitudinal cracks with about 94.6% and 92.3%, respectively. These recurrent neural network models have special advantages in providing strength and efficiency in detecting and classifying defects in road pavement. On the other hand, the supervised machine learning models, including RF, SVM, and DT, present acceptable results in identifying and classifying the longitudinal cracks among other distress types on the selected road at accuracies of about 85.8%, 84.2%, and 82.5%, respectively. Moreover, other model metrics such as precision, recall, and F1-score show high and significant values for each prediction model. This allows for the substantial use of the selected models in detecting and classifying pavement condition performance. Table 5 shows the performance of the recurrent neural network models and supervised machine learning models in predicting rutting on pavement surfaces at different spots on the selected road.

Table 5. Detection and classification of rutting using deep learning models

Model	Precision	Recall	F1 score	Accuracy
LSTM	91.55	91.21	91.37	91.44
GRU	91.02	90.83	90.92	90.27
RF	84.13	83.61	83.86	84.11
SVM	85.12	83.19	84.14	84.01
DT	82.62	81.04	81.82	81.25

According to Table 5, the prediction accuracies in detecting and classifying rutting were about 91.4% for using the LSTM model and about 90.3% for using the GRU model. The LSTM and GRU models' precision metric shows significant values in predicting the pavement condition in terms of rutting. Also, recall and F1-score values confirm the performance of the selected prediction models to detect and classify rutting. In contrast, the machine learning models provide acceptable accuracy ranges in predicting the functioning of pavement conditions in terms of detection and classification of the rutting cases among many different defect types.

In summary, all the prediction models demonstrate accurate detection and classification for normal cases (ideal pavement), with about 95.7% using LSTM, 95.4% for GRU, 94.8% for RF, 94.9% for SVM, and about 93.6% using DT. Besides, the results in Table 5 indicate that the artificial neural network models, including LSTM and GRU, were more efficient than the machine learning models, including RF, SVM, and DT, in terms of prediction, detection, and classification of the pavement conditions. The recurrent neural network (LSTM and GRU) uses a comprehensive detection and classification system, while the supervised machine learning models focus on using a binary system to detect and classify pavement degradation. Besides, the results indicate that the LSTM model was more significant in detecting and classifying the longitudinal cracks than other model types. In addition, the LSTM model was excellent in predicting the rutting cases, among many other defect types, on the selected road surface. Besides, the metric values of the LSTM model provided excellent ranges in the prediction of the pavement condition with a precision average of about 92% and about 91% for recall and F1-score, respectively.

Regarding the GRU, the model showed excellent ability to predict the condition of pavement surfaces in terms of existing longitudinal cracks and rutting with an overall accuracy of about 91%. Also, the average metric values of the GRU in the detection and classification of the pavement defects were about 91%, 90.6%, and 90.9% for precision, recall, and F1-score, respectively. At the same time, the results revealed that the longitudinal cracks and rutting were accurately predicted using the RF and SVM, with an overall prediction average of about 84.9% and 84.1%, respectively. Also, the high values of the models' metrics were provided at about 84.7% for precision, 83.3% for recall, and 84% for F1-score. Meanwhile, the SVM metrics values, including precision, recall, and F1-score, showed acceptable ranges of about 84.9%, 83.5%, and 84.2%, respectively. Finally, the DT models showed less accuracy than the previously selected prediction models, averaging 81.9% for detecting and classifying pavement distresses. The model metric values were close and corresponded to the accuracy target with about 83.2% for precision, 81.1% for recall, and 82.2% for F1-score. Figure 9 presents the loss, accuracy, and validation of the LSTM model.

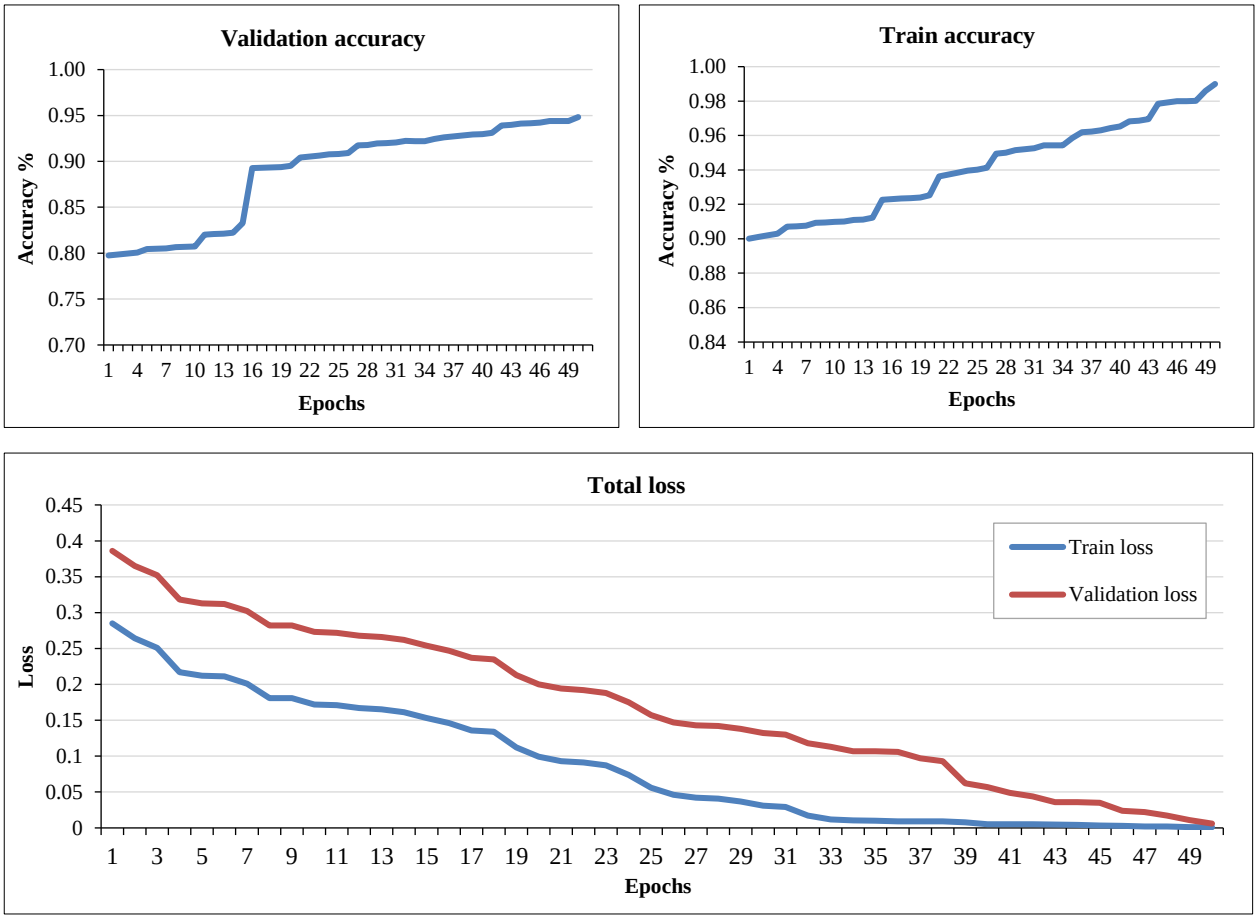

Figure 9. The loss and accuracy of the LSTM prediction model

Figure 9 presents the loss during the model development process, which indicates the LSTM model's behavior in detecting and classifying the pavement condition. Moreover, the train and validation accuracy are provided to show the model's performance in predicting the longitudinal cracks and rutting among other defect types on the selected road segment. Although all the prediction models provided accurate predictions for the three cases of pavement distress, the recurrent neural networks significantly predicted the pavement condition performance compared to the supervised machine learning models. The fluctuations in prediction accuracies between the neural network models and machine learning models are due to several reasons, including the fact that the machine learning models need large dataset sizes and limitations in variables and parameters. In addition, several factors may affect the accuracy of the proposed prediction models, such as the scanning location (set-up device spot), where the device was not fixed on a strength line along the selected road segment. More clearly, there were bit offsets during turning points from one position to another. Also, some longitudinal cracks were skinny and not clearly detected or measured using the laser scanner. Slight rutting cases were not detected as well due to a combination of two or more distress types at the same spots. Table 6 shows a comparison between the results of this research work and those of previous studies.

Table 6. Comparison between the results of this research work and those of previous studies

Work	Type of defects	Techniques	Performance	Detection Problem	Drawbacks/Limitations
Prasanna et al. (2012) [32]	Road defects	Support Vector Machines (SVM)	Accuracy (60%)	Detection	The outcomes indicated that the precision of practical predictions needed to be upgraded
Hoang & Nguyen (2019) [33]	Road defects	Support Vector Machines (SVM) and Random Forest (RF)	SVM (80.50%), followed by ANN (84.25%), then RF (70%).	Classification	Hard to detect rare types of damage
Mihoub et al. (2023) [38]	Smoothness, bumps, potholes, and others	Road Scanner and SVM classifier (Support Vector Machines)	Accuracy rate of 80.05%.	Detection	Hard to detect rare types of damage
Daneshvari et al. (2024) [40]	Bleeding	One-class support vector machine (SVM) algorithm	F1-score of 80.29%.	Detection	Doubles computational time
Daneshvari et al. (2024) [44]	Road defects	SVM	97.29 % in the testing dataset	Classification	Hard to detect rare types of damage
Zhang et al. (2018) [46]	Potholes, rutting, shoving	3D laser scanner	Detection accuracy above 78%.	Classification	Hard to detect rare types of damage
Azam et al. (2023) [47]	Cracking, rutting, roughness, and miscellaneous distresses	Terrestrial Laser Scanner (TLS)+PCI	Significant improvement in determining flexible pavement distresses and geometric characteristics	Classification	Hard to detect rare types of damage
Gopalakrishnan et al.(2017) [51]	Pavement longitudinal cracks	Transfer learning & VGG	Accuracy = 80%	Classification	Fails to learn to distinguish cracks from joints in PCC-surfaced pavements
Rajadurai and Kang (2021) [52]	Surface longitudinal cracks	AlexNet	Accuracy = 81–89%	Classification	Accuracy degraded by shadows, surface roughness, scaling, edges, holes, and background debris
Stricker et al. (2019) [53]	Road defects	GAN & Auto-decoder	Accuracy = 60%	Classification	The performance can be improved
Chaiyasarn (2014) [54]	Road defects	SSD	Precision > 75%	Classification	The performance can be improved
Present Study	Three main defect classes: longitudinal cracking; rutting and normal (ideal pavement spots).	Integration between potential 1- Terrestrial laser scanning systems 2- PCI Procedure for automated prediction, detection and classification of longitudinal cracks and rutting. 3- Deep Machine learning prediction models including (LSTM), (GRU), (RF), (SVM), (DT).	The prediction models showed significant accuracy with about 1-LSTM 93%, 2-GRU 91%, 3-RF 85%, 4-SVM 84%, 5- DT 82%,	Some longitudinal cracks were skinny and not clearly detected or measured using the laser scanner. Moreover, slight rutting cases were not detected due to a combination of two or more distress types at the same spots.	The fluctuations in prediction accuracies between the neural network models and machine learning models are due to several reasons, including the fact that the machine learning models need large dataset sizes and limitations in variables and parameters. In addition, several factors may affect the accuracy of the proposed prediction models, such as the scanning location (set-up device spot), where the device was not fixed on a strength line along the selected road segment. More clearly, there were bit offsets during turning points from one position to another.

Table 6 summarizes a sample of previous studies. Evidently, there are different methodologies for distress detection and classification, like laser scanner and image processing techniques, deep machine learning, and standard PCI procedures. Every methodology has its own unique characteristics regarding performance, accuracy, and standard deviation based on different factors like the type of distress to be detected, the methodology itself, and the drawbacks/limitations associated with it. In conclusion, each methodology is considered case dependent. As highlighted by Table 6, the novelty of this research work lies in the integration of different methodologies like terrestrial laser scanning systems, five deep machine learning prediction models, and traditional PCI procedures for validation. This integration allows detecting and classifying the required three main defect classes automatically and achieving excellent results with higher accuracies compared to previous studies due to the five deep machine learning prediction models.

4. Conclusion

This study focused on introducing a new pavement monitoring technique using a laser scanner device. The monitoring method aimed to evaluate the pavement conditions in terms of the existing two defect types: longitudinal cracking and rutting. The research also studied the use of the pavement condition index to evaluate the same pavement sections to validate the proposed monitoring technique. Besides, computation of the PCI depended on the visual condition survey in which distress type, severity, and quantity are evaluated for the distressed spots (as described in section 3.3) in order to verify the exact defect locations, types, and severities and to compare and validate the proposed monitoring technique. The PCI results indicated that the average PCI for 15 sample units of the longitudinal crack section is 48.13 (the PCI rate is poor), whereas the average PCI for 10 sample units of the rutting section is 37.3 (the PCI rate is very poor). Most of the severity levels were medium and high, as shown in Table 2, which indicates that these sections of the pavement need maintenance and rehabilitation.

After monitoring the pavement condition, several noise-canceling techniques were performed on the data to remove outliers and confirm that the data was clear and consistent. Subsequently, other processing techniques were applied using labeling technology to identify the locations of each type of pavement defect on the collected laser data. These pre-processing techniques were used to ensure greater quality in the pavement condition prediction process. The deep machine learning system was used to determine the efficiency of the measured data in identifying and classifying the types and severity of road defects using different machine learning models such as LSTM, GRU, RF, SVM, and DT. The results concluded that the LSTM and GRU models accurately detected and classified the two defect types among other types of pavement distresses located on the road segment. Finally, the other machine learning algorithms, including RF, SVM, and DT, provided acceptable ranges of prediction accuracies for the pavement defects.

Future studies could apply deep image processing techniques on the panoramic images taken by the laser device with the use of video recordings from a specialized camera to assess the condition of the road surface and automatically determine the type and severity of defect using a cellular application.

5. Declarations

5.1. Author Contributions

Conceptualization, B.A.M. and R.I.; methodology, B.A.M.; software, A.S.; validation, B.A.M., R.I., and A.S.; formal analysis, A.A.; investigation, R.I.; resources, A.A.; data curation, A.A.; writing—original draft preparation, B.A.M.; writing—review and editing, B.A.M., R.I., and A.S.; visualization, A.A.; supervision, B.A.M.; project administration, B.A.M.; funding acquisition, A.A. All authors have read and agreed to the published version of the manuscript.

5.2. Data Availability Statement

The data presented in this study are available on request from the corresponding author.

5.3. Funding

The authors received no financial support for the research, authorship, and/or publication of this article.

5.4. Conflicts of Interest

The authors declare no conflict of interest.

6. References

[1] Obaidat, M. T., Al-Suleiman, T. I., & Abdul-Jabbar, G. T. (1997). Quantification of Pavement Rut Depth Using Stereovision Technology. Journal of Surveying Engineering, 123(2), 55–70. doi:10.1061/(asce)0733-9453(1997)123:2(55).

[2] Al-Suleiman, T. I., Obaidat, M. T., Abdul-Jabbar, G. T., & Khedaywi, T. S. (2000). Field inspection and laboratory testing of highway pavement rutting. Canadian Journal of Civil Engineering, 27(6), 1109–1119. doi:10.1139/l00-037.

[3] Shahin, M. Y. (1994). Pavement Management for Airports, Roads, and Parking Lots. Springer, New York, United States. doi:10.1007/978-1-4757-2287-1.

[4] Oliveira, H. J. M. (2013). Crack detection and characterization in flexible road pavements using digital image processing. Instituto Superior Tecnico, Lisbon, Portugal.

[5] Meignen, D., Bernadet, M., & Briand, H. (1997). One application of neural networks for detection of defects using video data bases: identification of road distresses. Database and Expert Systems Applications. 8th International Conference, DEXA '97. Proceedings, 459–464. doi:10.1109/dexa.1997.617332.

[6] Cheng, H. D., & Miyojim, M. (1998). Automatic pavement distress detection system. Information Sciences, 108(1–4), 219–240. doi:10.1016/S0020-0255(97)10062-7.

[7] Subirats, P., Fabre, O., Dumoulin, J., Legeay, V., & Barba, D. (2004). A combined wavelet-based image processing method for emergent crack detection on pavement surface images. 2004 12th European signal processing conference, 6-10 September, 2004, Vienna, Austria.

[8] Beraldin, J. A., Blais, F., & Lohr, U. (2010). Laser Scanning Technology. Airborne and Terrestrial Laser Scanning, Whittles Publishing, London, United Kingdom.

[9] Wang, K. C. P. (2000). Designs and Implementations of Automated Systems for Pavement Surface Distress Survey. Journal of Infrastructure Systems, 6(1), 24–32. doi:10.1061/(asce)1076-0342(2000)6:1(24).

[10] Zhang, W., Zhang, Z., Qi, D., & Liu, Y. (2014). Automatic crack detection and classification method for subway tunnel safety monitoring. Sensors (Switzerland), 14(10), 19307–19328. doi:10.3390/s141019307.

[11] Zhang, L., Yang, F., Daniel Zhang, Y., & Zhu, Y. J. (2016). Road crack detection using deep convolutional neural network. 2016 IEEE International Conference on Image Processing (ICIP), 3708–3712. doi:10.1109/icip.2016.7533052.

[12] Shatnawi, N. (2018). Automatic pavement cracks detection using image processing techniques and neural network. International Journal of Advanced Computer Science and Applications, 9(9), 399–402. doi:10.14569/ijacsa.2018.090950.

[13] Hoffmeister, D. (2020). Geological Records of Tsunamis and Other Extreme Waves. Elsevier, Amsterdam, Netherlands. doi:10.1016/c2017-0-03458-4

[14] Shan, J., & Toth, C. K. (2017). Topographic Laser Ranging and Scanning. CRC Press, Boca Raton, United States. doi:10.1201/9781420051438.

[15] Dickmanns, E. D., & Mysliwetz, B. D. (1992). Recursive 3-D Road and Relative Ego-State Recognition. IEEE Transactions on Pattern Analysis and Machine Intelligence, 14(2), 199–213. doi:10.1109/34.121789.

[16] Tao, C. V., & Li, J. (2007). Advances in Mobile Mapping Technology. CRC Press, London, United Kingdom. doi:10.4324/9780203961872.

[17] Al-Durgham, K., Lichti, D. D., Kwak, E., & Dixon, R. (2021). Automated accuracy assessment of a mobile mapping system with lightweight laser scanning and mems sensors. Applied Sciences (Switzerland), 11(3), 1–14. doi:10.3390/app11031007.

[18] Haala, N., Peter, M., Cefalu, A., & Kremer, J. (2008). Mobile LIDAR mapping for urban data capture. Proceedings of the 14th International Conference on Virtual Systems and Multimedia, 20-25 October, 2008, Limassol, Cyprus.

[19] Tsai, Y., Ai, C., Wang, Z., & Pitts, E. (2013). Mobile cross-slope measurement method using LIDAR technology. Transportation Research Record, 2367(2367), 53–59. doi:10.3141/2367-06.

[20] Campbell, D. M. H., White, B., & Arp, P. A. (2013). Modeling and mapping Soil resistance to penetration and rutting using LiDAR-derived digital elevation data. Journal of Soil and Water Conservation, 68(6), 460–473. doi:10.2489/jswc.68.6.460.

[21] Obaidat, M. T., Shatnawi, N., & Al-Sharideah, A. (2021). Geomatics techniques for evaluation of road pavement rutting. Applied Geomatics, 13(2), 217–225. doi:10.1007/s12518-020-00337-0.

[22] Hu, Y., Zhao, C., & Wang, H. (2010). Automatic Pavement Crack Detection Using Texture and Shape Descriptors. IETE Technical Review, 27(5), 398. doi:10.4103/0256-4602.62225.

[23] Cord, A., & Chambon, S. (2012). Automatic Road Defect Detection by Textural Pattern Recognition Based on AdaBoost. Computer-Aided Civil and Infrastructure Engineering, 27(4), 244–259. doi:10.1111/j.1467-8667.2011.00736.x.

[24] Shi, Y., Cui, L., Qi, Z., Meng, F., & Chen, Z. (2016). Automatic road crack detection using random structured forests. IEEE Transactions on Intelligent Transportation Systems, 17(12), 3434–3445. doi:10.1109/TITS.2016.2552248.

[25] Liu, F., Liu, J., & Wang, L. (2022). Deep learning and infrared thermography for asphalt pavement crack severity classification. Automation in Construction, 140, 104383. doi:10.1016/j.autcon.2022.104383.

[26] Shtayat, A., Moridpour, S., Best, B., & Abuhassan, M. (2023). Using supervised machine learning algorithms in pavement degradation monitoring. International Journal of Transportation Science and Technology, 12(2), 628–639. doi:10.1016/j.ijtst.2022.10.001.

[27] Kim, E., Jang, W. J., Kim, W., Park, J., Lee, M. K., Park, S. H. K., & Choi, K. C. (2016). Suppressed Instability of a-IGZO Thin-Film Transistors Under Negative Bias Illumination Stress Using the Distributed Bragg Reflectors. IEEE Transactions on Electron Devices, 63(3), 1066–1071. doi:10.1109/TED.2015.2513414.

[28] Sun, L., Kamaliardakani, M., & Zhang, Y. (2016). Weighted Neighborhood Pixels Segmentation Method for Automated Detection of Cracks on Pavement Surface Images. Journal of Computing in Civil Engineering, 30(2), 1–11. doi:10.1061/(asce)cp.1943-5487.0000488.

[29] Akagic, A., Buza, E., Omanovic, S., & Karabegovic, A. (2018). Pavement crack detection using Otsu thresholding for image segmentation. 2018 41st international convention on information and communication technology, electronics and microelectronics (MIPRO), 21-25 May, 2018, Opatija, Croatia.

[30] Sari, Y., & Prakoso, P. B. (2018). Detection of Moving Vehicle using Adaptive Threshold Algorithm in Varied Lighting. 2018 5th International Conference on Electric Vehicular Technology (ICEVT), 136–141. doi:10.1109/icevt.2018.8628398.

[31] Prakoso, P. B., & Sari, Y. (2019). Vehicle detection using background subtraction and clustering algorithms. Telkomnika (Telecommunication Computing Electronics and Control), 17(3), 1393–1398. doi:10.12928/TELKOMNIKA.V17I3.10144.

[32] Prasanna, P., Dana, K., Gucunski, N., & Basily, B. (2012). Computer-vision based crack detection and analysis. Sensors and Smart Structures Technologies for Civil, Mechanical, and Aerospace Systems 2012. doi:10.1117/12.915384.

[33] Hoang, N. D., & Nguyen, Q. L. (2019). A novel method for asphalt pavement crack classification based on image processing and machine learning. Engineering with Computers, 35(2), 487–498. doi:10.1007/s00366-018-0611-9.

[34] Gavilán, M., Balcones, D., Marcos, O., Llorca, D. F., Sotelo, M. A., Parra, I., Ocaña, M., Aliseda, P., Yarza, P., & Amírola, A. (2011). Adaptive road crack detection system by pavement classification. Sensors, 11(10), 9628–9657. doi:10.3390/s111009628.

[35] Chen, X., Yongchareon, S., & Knoche, M. (2023). A review on computer vision and machine learning techniques for automated road surface defect and distress detection. Journal of Smart Cities and Society, 1(4), 259–275. doi:10.3233/scs-230001.

[36] Finogeev, A., Deev, M., Finogeev, A., & Parygin, D. (2024). Recognition and Clustering of Road Pavement Defects by Deep Machine Learning Methods. Machine Learning Methods in Systems, CSOC 2024, Lecture Notes in Networks and Systems, 1126, Springer, Cham, Switzerland. doi:10.1007/978-3-031-70595-3_48.

[37] Hassan, S., O'sullivan, D., Mckeever, S., Power, D., Mcgowan, R., & Feighan, K. (2022). Detecting Patches on Road Pavement Images Acquired with 3D Laser Sensors using Object Detection and Deep Learning. Proceedings of the 17th International Joint Conference on Computer Vision, Imaging and Computer Graphics Theory and Applications. doi:10.5220/0010830000003124.

[38] Mihoub, A., Krichen, M., Alswailim, M., Mahfoudhi, S., & Bel Hadj Salah, R. (2023). Road Scanner: A Road State Scanning Approach Based on Machine Learning Techniques. Applied Sciences (Switzerland), 13(2). doi:10.3390/app13020683.

[39] Cui, P., Bidzikrillah, N. A., Xu, J., & Qin, Y. (2024). Application of the Semi-Supervised Learning Approach for Pavement Defect Detection. Sensors, 24(18). doi:10.3390/s24186130.

[40] Daneshvari, M. H., Mojaradi, B., Ameri, M., & Nourmohammadi, E. (2024). Automation detection of asphalt pavement bleeding for imbalanced datasets using an anomaly detection approach. Measurement: Journal of the International Measurement Confederation, 235, 114987. doi:10.1016/j.measurement.2024.114987.

[41] Han, C., Yang, H., Ma, T., Wang, S., Zhao, C., & Yang, Y. (2024). Crack Diffusion: A two-stage semantic segmentation framework for pavement crack combining unsupervised and supervised processes. Automation in Construction, 160, 105332. doi:10.1016/j.autcon.2024.105332.

[42] Isradi, M., Rifai, A. I., Prasetijo, J., Kinasih, R. K., & Setiawan, M. I. (2024). Development of Pavement Deterioration Models Using Markov Chain Process. Civil Engineering Journal (Iran), 10(9), 2954–2965. doi:10.28991/CEJ-2024-010-09-012.

[43] Zafar, M. S., Shah, S. N. R., Memon, M. J., Rind, T. A., & Soomro, M. A. (2019). Condition Survey for Evaluation of Pavement Condition Index of a Highway. Civil Engineering Journal (Iran), 5(6), 1367–1383. doi:10.28991/cej-2019-03091338.

[44] Daneshvari, M. H., Mojaradi, B., Ameri, M., & Nourmohammadi, E. (2024). Hybrid texture analysis of 2D images for detecting asphalt pavement bleeding and raveling using tree-based ensemble methods. Alexandria Engineering Journal, 107, 150-164. doi:10.1016/j.aej.2024.07.028.

[45] Zhang, D., Zou, Q., Lin, H., Xu, X., He, L., Gui, R., & Li, Q. (2018). Automatic pavement defect detection using 3D laser profiling technology. Automation in Construction, 96, 350–365. doi:10.1016/j.autcon.2018.09.019.

[46] Chow, J. C. (2014). Multi-sensor integration for indoor 3D reconstruction. Doctoral dissertation, University of Calgary, Calgary, Canada.

[47] Azam, A., Alshehri, A. H., Alharthai, M., El-Banna, M. M., Yosri, A. M., & Beshr, A. A. A. (2023). Applications of Terrestrial Laser Scanner in Detecting Pavement Surface Defects. Processes, 11(5), 1370. doi:10.3390/pr11051370.

[48] Zheng, L., Xiao, J., Wang, Y., Wu, W., Chen, Z., Yuan, D., & Jiang, W. (2024). Deep learning-based intelligent detection of pavement distress. Automation in Construction, 168. doi:10.1016/j.autcon.2024.105772.

[49] Riid, A., Lõuk, R., Pihlak, R., Tepljakov, A., & Vassiljeva, K. (2019). Pavement distress detection with deep learning using the orthoframes acquired by a mobile mapping system. Applied Sciences (Switzerland), 9(22), 4829. doi:10.3390/app9224829.

[50] Shahin, M. Y., & Walther, J. a. (1990). Pavement Maintenance Management for Roads and Streets Using the PAVER System No. CERL-TR-M-90/05. US Army Corps of Engineers, Construction Engineering Research Laboratory, Washington, United States.

[51] Gopalakrishnan, K., Khaitan, S. K., Choudhary, A., & Agrawal, A. (2017). Deep Convolutional Neural Networks with transfer learning for computer vision-based data-driven pavement distress detection. Construction and Building Materials, 157, 322–330. doi:10.1016/j.conbuildmat.2017.09.110.

[52] Rajadurai, R. S., & Kang, S. T. (2021). Automated vision-based crack detection on concrete surfaces using deep learning. Applied Sciences (Switzerland), 11(11), 5229. doi:10.3390/app11115229.

[53] Stricker, R., Eisenbach, M., Sesselmann, M., Debes, K., & Gross, H.-M. (2019). Improving Visual Road Condition Assessment by Extensive Experiments on the Extended GAPs Dataset. 2019 International Joint Conference on Neural Networks (IJCNN), 1–8. doi:10.1109/ijcnn.2019.8852257.

[54] Chaiyasarn, K. (2014). Damage detection and monitoring for tunnel inspection based on computer vision. Ph.D. Thesis, University of Cambridge, Cambridge, United Kingdom.